The Computational Modelling the Short Crack Fatigue Behaviour of Al-SiC MMCs

M. S. Bruzzi and P. E. McHugh
Department of Mechanical Engineering,
National University of Ireland, Galway, Ireland.

Abstract

The objective of this study is to develop a computational modelling methodology of the fatigue crack growth behaviour of: (1) a forged 2124 Al reinforced with 17% SiC particles and (2) a cast 359 Al reinforced with 20% SiC particles. In particular, the focus of this work is on correlating local crack tip driving force conditions of an initial short crack with an experimental long crack growth rate curve, using crack closure. A defect tolerant approach is assumed. The crack tip is modelled using the finite element method, and the correlating parameter, ΔJ_{eff} (the effective range of the J-integral), is calculated. The material is assumed to be homogenous with the macroscale properties of the metal matrix composite, (MMC), for modelling purposes. An effective crack growth rate curve is calculated, and the ΔJ is used to obtain the crack growth increment per cycle. The method is repeated with the new crack size until the entire crack growth rate curve for the initial short crack is obtained. Crack growth rate curves for different stress levels and initial defect sizes are presented. Predicted S-N curves, obtained from the crack growth rate curves for a loading ratio of R=0.1, are compared with experimental results for each of the particulate reinforced MMCs. A good agreement with experimental results is obtained for an appropriate choice of defect size.

Introduction

Since Pearson (1975) [1] first reported the so-called anomalous behaviour of small fatigue cracks, it has been well established that the growth rates of small cracks can exceed those of large cracks at theoretically equivalent stress-intensity ranges, ΔK, [2-5]. Also, it is accepted that small cracks can propagate at stress intensities less than the fatigue threshold, ΔK_{th}, below which large crack growth is presumed not to occur.

Small cracks can be further classified as *microstructurally-small cracks*, *mechanically small cracks* or *physically small* (or short) *cracks* [6]. Microstructurally small cracks are cracks whose dimensions are on the order of the material microstructure, e.g. grain size, and where local crack growth rates may accelerate along 'weak paths' or decelerate or even arrest at microstructural barriers. Mechanically small cracks is the term used to describe cracks where the local crack tip plastic zone size is large rendering the linear elastic fracture mechanics assumption of small scale yielding invalid. Physically small, also called short cracks, usually describe through thickness cracks where reduced crack closure leads to a higher local driving forces than the corresponding long crack with the same nominal applied ΔK. The behaviour of all the above small cracks can lead to serious non-conservative

predictions of fatigue life, since most defect tolerant fatigue lifetime estimations are based on long crack data.

Many modelling approaches have been published, attempting to model and interpret the small crack problem. Among these, many have interpreted the behaviour mechanisms of microstructurally small cracks to be fundamentally different to those of the short crack [7]. The behaviour of microstructurally small cracks has been modelled assuming a reduction in the local crack tip driving force due to an interaction with features of the material microstructure, such as a grain boundary [8]. The experimentally observed retardation and arrest of small cracks, after initial rapid growth rates, has been attributed mainly to biased statistical sampling involving microstructural barriers impeding local crack growth [7]. Crack closure has been proposed as the responsible mechanism for the physically short crack phenomenon, and the use of the effective crack tip stress intensity range, ΔK_{eff}, helps explain the short crack behaviour. The use of correlating parameters such as ΔJ and the crack tip opening displacement, CTOD, have been used along with crack closure as potential solutions in explaining and predicting the behaviour of mechanically small cracks [6].

In this work, a methodology is developed using the effective range of the J-integral, ΔJ_{eff}, to characterise the elastic-plastic fatigue crack growth (EPFCG) behaviour of an initial short crack [9]. Experimentally determined closure levels are considered and crack growth rate curves for an initial short crack in each of the MMCs are presented for varying stress levels. By using the EPFCG correlating parameter ΔJ_{eff}, which takes closure into consideration, both mechanically small cracks and physically short cracks can be modelled using the same methodology. The use of crack closure in explaining the crack growth rates of microstructurally small cracks is also examined and discussed. Finally, predicted S-N curves are compared with experimental results for each of the particulate reinforced MMCs, at an R-ratio of 0.1.

Methodology

This methodology for modelling the growth behaviour of a short crack and resulting fatigue behaviour assumes a defect tolerant approach, i.e. an initial flaw, free of crack closure, exists in the material. It is the propagation of this initial crack under cyclic loading which is assumed to constitute the fatigue behaviour of the material. The material of interest for development and validation of the methodology are: (1) a forged 2124 Al reinforced with 17% SiC particles and (2) a cast 359 Al reinforced with 20% SiC particles.

The elastic-plastic fracture mechanics parameter, J, which is now widely accepted as an appropriate parameter to characterise elastic-plastic crack growth under monotonic loading, is (for power-law materials) often given by [9]:

$$J = \frac{K^2}{E'}\left\{1 + \frac{F^2}{C_2}\left(\frac{n-1}{n+1}\right)\left[\frac{(\sigma_\infty/\sigma_0)^2}{1+(\sigma_\infty/\sigma_0)^2}\right]\right\} + \alpha\sigma_0\varepsilon_0 a h_1\left(\frac{\sigma_\infty}{\sigma_0}\right)^{n+1} \quad (1)$$

where C_2 = 6 for plain strain. F is defined as the collective geometry term in the elastic K expression,

$$K = F\sigma_\infty\sqrt{\pi a} \quad (2)$$

σ_∞ is the applied far-field stress and a is the crack length. The effective elastic modulus, E', is equal to $E/(1-\nu^2)$ for plane strain, where E is Young's modulus and ν

is Poisson's ratio. The Ramberg-Osgood (power-law) constitutive relationship is defined by the strain hardening exponent, n, and the coefficients α, ε_0 and σ_0. In one dimension this takes the form:

$$\frac{\varepsilon}{\varepsilon_0} = \frac{\sigma}{\sigma_0} + \alpha\left(\frac{\sigma}{\sigma_0}\right)^n \tag{3}$$

The analogue to Eq. (1) for cyclic loading is given by ΔJ, which as pointed out by Lamba and others, [10-12], comprises of the monotonic J expression with the single value of σ_∞ in K replaced by its range, $\Delta\sigma_\infty$, in ΔK [9]. Also, the second term on the right hand side of Eq. (1) was modified to correct for the effects of reversed deformation [9]. In order to include corrections for plasticity-induced crack closure, ΔJ_{eff} is concluded to be a more appropriate correlating parameter of EPFCG, [13], and is given by:

$$\Delta J_{eff} = \frac{(U\Delta K)^2}{E'}\left\{1 + \frac{F^2}{C_2}\left(\frac{n-1}{n+1}\right)\left[\frac{\left(\sigma_\infty^{max}/\sigma_0\right)^2}{1+\left(\sigma_\infty^{max}/\sigma_0\right)^2}\right]\right\} + 4\alpha\sigma_0\varepsilon_0 a h_1 U\left(\frac{\Delta\sigma_\infty}{2\sigma_0}\right)^{n+1} \tag{4}$$

where U is the effective stress range ratio,

$$U = \frac{\sigma_{max} - \sigma_{open}}{\sigma_{max} - \sigma_{min}} \tag{5}$$

σ_{open} is the stress at which the crack surfaces become completely separated, during loading. $\sigma_{open} \geq \sigma_{min}$ due to crack closure.

Crack closure was quantified by the use of an experimental resistance curve for the threshold of fatigue propagation [14,15], which gave a plot of crack extension, against the stress intensity range threshold, ΔK_{th}. Firstly, the minimum stress range $\Delta\sigma=\sigma_{max}-\sigma_{min}$ for the growth of a long crack of length a, for a given stress ratio, $R=\sigma_{min}/\sigma_{max}$, using the long crack threshold, $\Delta K_{th,lc}$, was calculated. σ_{open} was then calculated using the short crack threshold for the given extension, as obtained from the resistance curve of the MMC.

The Ramberg-Osgood power-law constitutive relationship, described above, was fitted to the calculated true tensile stress (σ_{true}) – logarithmic strain (ε_{true}) curve, obtained from tensile test data for each of the MMCs [16]. The strain hardening exponent, n, and the coefficients α, ε_0 and σ_0 were then evaluated for each MMC.

The only undetermined quantity in order to be able to numerically calculate the value of ΔJ_{eff} for a given crack length, a, was h_1 which is a function of both the constitutive relationship and the crack length. By performing a finite element simulation of a specimen under tensile loading with an initial crack loaded to a stress σ_{max}, the J-integral around the crack tip was obtained and hence h_1 was determined from Eq. (1).

In the finite element simulations, the initial flaw was assumed to be a sharp crack (where the crack faces lie on top of each other in the undeformed configuration) of length a_0 and free of closure. Simulations were performed which incorporated elastic and elastic-plastic constitutive laws in the context of finite deformation kinematics. The MMC was assumed to be homogenous, with the material properties of the composite, for modelling purposes. Elasticity was considered as being isotropic and linear in terms of finite deformation quantities [17]. Plasticity was described by isotropic hardening, rate independent, J_2 flow theory. The elastic constants and the plastic strain hardening properties of each MMC were determined from the calculated tensile σ_{true}-ε_{true} curve obtained from the tensile test data [16]. For symmetry reasons,

it was only necessary to model one half of the surface crack. The specimen modelled had a length one hundred times greater than that of the crack, so that no boundary effects would be encountered. A 2D plane strain analysis was performed, and so the 2D crack represented a through thickness physically small crack. Focussed 8-noded quadrilateral elements, where one side of each element was collapsed so that all three nodes had the same geometrical location, were used to model the crack tip singularity, [18]. A uniformly distributed vertical tensile stress was applied to the top surface.

Once h_1 was determined for a given crack length, ΔJ_{eff} could then be calculated for any loading condition, and could be used to quantify the local crack tip driving force. This correlating parameter is satisfactory for both mechanically small and physically short cracks through the use of elastic-plastic fracture mechanics and the consideration of crack closure in ΔJ_{eff}, respectively.

It was necessary to correlate ΔJ_{eff} with the rate at which the crack would grow if subjected to this driving force. Since $\Delta K_{th,lc}$ is independent of crack length, a, for long cracks, it was assumed that closure remains constant for a propagating long crack. The effect of closure was then removed by multiplying the long crack growth rate curve by $U = \Delta K_{th,eff} / \Delta K_{th,lc}$, where $\Delta K_{th,eff}$ is the threshold for growth of a short crack, to obtain an effective crack growth rate curve i.e. da/dN versus ΔK_{eff}.

Assuming linear elastic fracture mechanics was valid for the experimental long crack growth rate curve, the crack tip driving force, ΔK_{eff}, was then correlated with ΔJ_{eff}, and was calculated from:

$$\Delta K_{eff} = \sqrt{\Delta J_{eff} E'} \tag{6}$$

The crack growth rate da/dN and the increment of crack extension for one cycle, a_{ext} was then obtained from the effective crack growth rate curve. The procedure was repeated for the new crack length a + a_{ext}. The specimen was assumed to have failed when ΔK_{eff} reached the maximum value of ΔK in the long crack growth rate curve for each material.

Results

The crack growth rate curves for initial short cracks of length, a_0, were calculated by the methodology described above, for each of the MMCs for an R-ratio of 0.1 and with different applied stress levels.

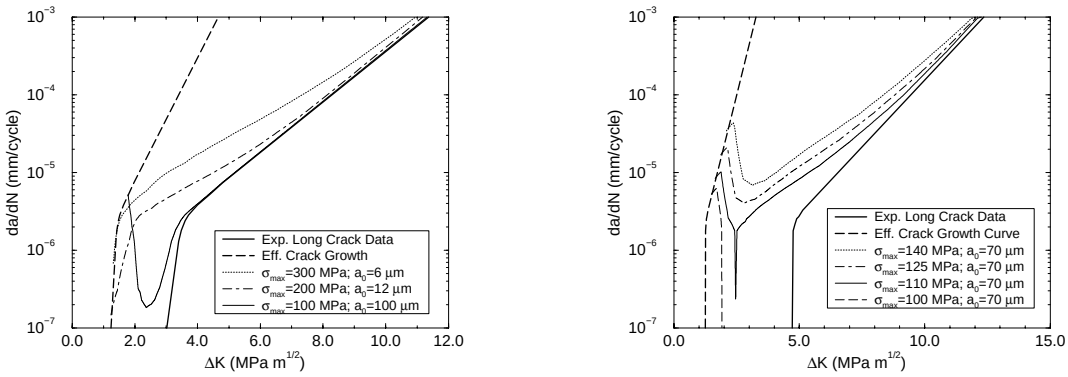

(a) (b)

Figure 1: Crack growth rate curves at R=0.1 for: (a) Al 2124 + 17% SiC, (b) Al 359 + 120% SiC.

Figure 1 (a) and (b) shows ΔK plotted against da/dN for the Al 2124 MMC and the Al 359 MMC, respectively. Also shown in Figure 1 is the calculated effective crack growth rate curve for each MMC.

It can be seen in Figure 1 (a) that the initial small crack starts to grow, due to a lack of crack closure, at a rate dictated by the effective crack growth rate curve. For high maximum stress levels and low initial crack sizes, the crack growth rate increases steadily with increasing ΔK, and the level of crack closure increases with increasing crack length. As the calculated crack extension approaches the length of a long crack, the closure reaches a steady state value and so the short crack growth rate curve approaches that of a long crack. This is typical of the behaviour of mechanically small and physically short cracks as described by Lankford and Davidson, [7].

If, however, a_0 has a large value (typically >50μm), and the applied stress is low, the initial increase in ΔK_{th}, due to crack closure, may be much greater than the increase in the crack tip driving force, ΔJ_{eff}, due to the extension of the crack by a_{ext}. This causes the crack growth rate to decrease from an initially high crack growth rate, until the increase in ΔK_{th} is less than the increase in ΔJ_{eff}, for a calculated a_{ext}. This is shown in Figure 1 (a) and (b). It can also be seen that the crack may arrest as shown in Figure 1 (b) (for a_0=70μm and σ_{max}=100Mpa) or may decrease to a minimum value and then gradually increase. This is typical of the behaviour of microstructurally small cracks as described by Lankford and Davidson [7].

The number of cycles required for an initial crack to grow at a rate of 10^{-3} mm/cycle was calculated for a given a_0 for each material, and for a range of stress levels at R=0.1. At this growth rate, the material was assumed to propagate rapidly to failure. The S-N curve as calculated using the methodology described in this work, is shown for both the Al 2124 MMC and the Al 359 MMC in Figure 2 (a) and (b), respectively. The experimental data, [15], is also shown.

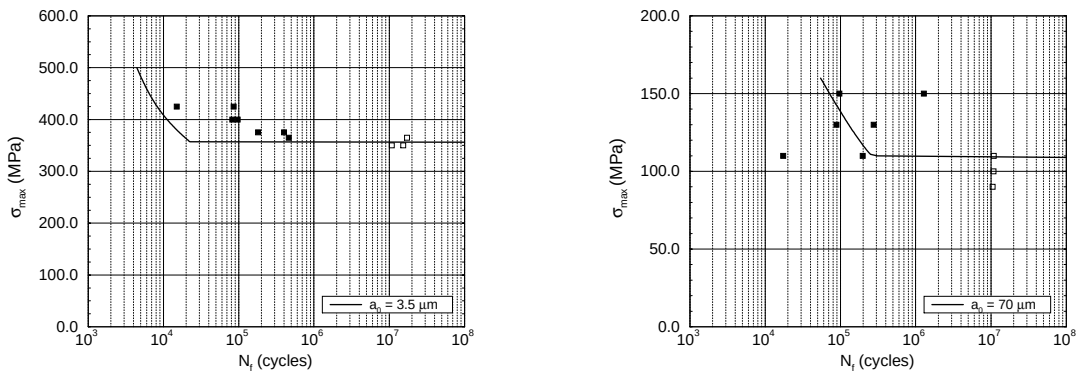

(a) (b)

Figure 2: S-N curves at R=0.1 for: (a) Al 2124 + 17% SiC and (b) Al 359 + 120% SiC.

It is clearly seen that a choice of a_0=3.5μm gives a good fit for the Al 2124 MMC, which is typical of the defect sizes found in this material [15]. It does, however, give a conservative prediction at the higher stress levels of the S-N curve. A choice of a_0=70μm gives a good fit for the Al 359 MMC, although there is much greater scatter in the experimental data. This is also typical of the defect sizes which exist in the cast MMC [15].

For both MMCs, a definite fatigue limit exists. This is due to the assumption, within the methodology, that a crack will only grow if the effective crack tip driving force exceeds the threshold stress intensity factor range, ΔK_{th}, for a corresponding length of crack growth.

Discussion and Conclusions

This methodology uses the elastic-plastic fracture mechanics correlating parameter ΔJ_{eff} to quantify the crack tip driving force of a propagating small crack. This correlating parameter is valid for both mechanically small and physically short cracks through the use of elastic-plastic fracture mechanics and the consideration of crack closure, respectively. The methodology models and explains the fatigue crack growth rates of both mechanically small and physically short cracks, as detailed in [7], through the use of crack closure, and on a cycle by cycle basis. The methodology also helps explain, quantitatively, the 'anomalous' decreasing behaviour (and possible arrest) of microscopically small cracks, directly through the use of crack closure and not through the use of microstructural 'barriers'. The effects of these microstructural barriers are, however, intrinsic in the experimental resistance curve for quantifying crack closure.

The method also gives an accurate prediction of the S-N behaviour of each MMC for an appropriate choice of a_0. The initial flaw size is critical for the accurate prediction of the S-N curve for each of the MMCs. However, despite the choice of a_0, to give an accurate fit to the experimental data, the general S-N curve trend is maintained, and a defined fatigue limit is determined.

Acknowledgements

The author thanks all partners of the BRITE/EURAM project MISPOM (Aerospatiale Matra, Defence Evaluation and Research Agency, Universitat Politenica de Catalunya, Università di Ancona, Erich Schmid Institut, TEKSID, National University of Ireland, Galway) for their collaboration. They are indebted to the European Community for financial support.

References

[1] Pearson, S., *Eng. Fract.Mech.*, **7**, 1975, pp. 235-247.
[2] Miller, K.J., *Fat. Eng. Mater. Struct.*, **5**, 1982, pp. 223-232.
[3] Suresh, S. and Ritchie, R.O., *Int. Metals Reviews*, **29**, 1984, pp. 445-478.
[4] Miller K.J, and De Los Rios, E.R. eds., The behaviour of short fatigue cracks, Mech. Eng. Publ., London, U.K., 1986.
[5] Lankford, J., *Fatigue Eng. Mat. Struc.*, **5**, 1982, pp. 233-248.
[6] Ritchie, R.O. and Lankford, J., *Mater. Sci. Eng.*, **84**, 1996, pp.11-16.
[7] Lankford, J. and Davidson, D.L., Proceedings of the second international workshop on small fatigue cracks, 1986, Santa Barbara, California.
[8] Tanaka, K., Small Fatigue Cracks, 1987, pp.343-361.
[9] McClung, R.C., Chell, G.G., Russel, D.A. and Orient, G.E., *Fatigue and Fracture Mechanics*, **27**, ASTM STP 1296, R.S. Piascik, J.C. Newman and N.E. Dowling, EDS., 1997, pp.317-337

[10] Lamba, H.S., *Eng. Fract. Mech*, **7**, 1975, pp. 693-703.
[11] Withrich, C., *International Journal of Fracture*, **20**, 1982, pp. R35-R37.
[12] Tanaka, K., *International Journal of Fracture*, **22**, 1983, pp. 91-104.
[13] McClung, R.C. and Sehitoglu, H., *ASME Journal of Eng. Maters. And Tech.*, **113**, 1991, pp. 15-22.
[14] Tabernig, B. and Pippan, R., Proceedings of the seventh international fatigue congress. Eds. X.R. Wu and Z.G. Wang, 1999, **3**, pp. 1477-1482.
[15] Tabernig, B. and Pippan, R., Submission to Fatigue 2000: Eight international fatigue congress.
[16] Forn, A., Private Communication, 1998.
[17] *ABAQUS Theory Manual*. (1997a) HKS Inc., Providence, RI, USA.
[18] *ABAQUS User's Manual*. (1997b) HKS Inc., Providence, RI, USA.